Proceedings IRG Annual Meeting (ISSN 2000-8953)

IRG/WP 26-41056

THE INTERNATIONAL RESEARCH GROUP ON WOOD PROTECTION

Section 4 **Applications and Performance**

Update on timber decay hazard map of Australia

Chandan Kumar, Lesley Francis, Babar Hassan, & Jack Dorries

[1] Department of Primary Industries, Queensland Government
50 Evans Road, Salisbury, QLD, 4107, Australia

Paper prepared for the IRG56 Scientific Conference on Wood Protection
Beijing, China
24 – 28 May, 2026

IRG SECRETARIAT
Drottning Kristinas v. 61B
SE-114 28 Stockholm
Sweden
www.irg-wp.com

Update on timber decay hazard map of Australia

Chandan Kumar[1], Lesley Fancis[1], Babar Hassan[1], & Jack Dorries[1]

[1] Department of Primary Industries, Queensland Government, 50 Evans Road, Salisbury, QLD, 4107, Australia
Emails: chandan.kumar@dpi.qld.gov.au; lesley.francis@dpi.qld.gov.au; babar.hassan@dpi.qld.gov.au; jack.dorries@dpi.qld.gov.au.

ABSTRACT

Timber durability in outdoor applications is strongly influenced by climatic conditions such as rainfall, temperature, and humidity, which affect the activity of biodeteriogens. Existing Australian service life prediction models rely on empirical climate relationships, based on rainfall, temperature and dry days, which were drawn upon to formulate hazard map zones that were then set with expert guidance. The current hazard maps developed in the Forest & Wood Products Australia Design for Durability (FWPA DfD) project divide Australia into four broad hazard zones, that were convenient to use and represented the best approach at the time. Areas that experience quite different decay hazards, however, may fall within the same zone, and locations either side of zone boundaries can appear to have abrupt changes in decay potential. This limits the accuracy of the maps and calculations that rely on zone factors, and highlights the need for a more detailed, location-specific approach drawing on information technology resources now available. This paper presents decay hazard maps for Australia that were developed using multiple approaches, followed by a comparative overview and discussion of their outcomes. The analysis began with the Scheffer Climate Index (SCI), a widely used indicator of above-ground decay potential based on mean monthly temperature and rainfall. The report then discusses hazard maps that were produced using the Department of Primary Industries Durability Index (DI), which incorporates drying potential through vapour pressure deficit and percent wet days (factors particularly relevant to Australian climates). Finally, in-ground hazard maps based on equations developed in the FWPA DfD project were presented, alongside an assessment of the limitations of applying the FWPA DfD equation to above-ground conditions and the proposal of a new approach. Each hazard mapping approach demonstrated strengths and limitations. For example, the SCI may underrepresent decay potential in southern Western Australia and in regions near, but not adjacent to the coast, while the DI provides better representation in WA but may overestimate decay hazards in Tasmania. The published FWPA DfD hazard maps categorise Australia into four broad zones. In this paper, a higher-resolution hazard map based on FWPA DfD formulae for in-ground applications was produced. For above-ground environments, due to complexity in the half-hourly rainfall data, maps were generated using a generalised linear model (GLM) that incorporated variables such as mean annual temperature, average annual vapour pressure deficit, and average daily rainfall. Enhanced maps can be made publicly accessible once verification and validation are completed. With modern data-visualisation tools, an online platform incorporating heat maps and location-specific "pin-drop" queries will provide an effective and user-friendly means of determining climate hazard values for any selected Australian location.

Keywords: Durability, decay, termite damage, hazard map, climate, timber assessment.

1. INTRODUCTION

There is increasing interest in the use of timber within the building and construction industry due to its low carbon footprint, renewability, and use as a natural and sustainable building resource.

Beyond its environmental advantages, timber offers several practical benefits: it is lightweight, cost-effective, thermally insulating, visually appealing, and more resistant to corrosion in saline or acidic environments compared to most metals. However, timber is a biological material and is therefore susceptible to deterioration.

Timber deterioration results from a combination of biotic agents (such as decay fungi, bacteria and wood-boring insects) and abiotic factors (including ultraviolet radiation, wetting and drying cycles). Climate plays a major role by influencing the activity of biodeteriogens, and has long been recognised as a key determinant of timber durability in outdoor applications (Eaton and Hale 1993, Rayner and Boddy 1988, Zabel and Morrell 2020). In addition, construction design, moisture protection and maintenance practices strongly influence wetting exposure and can extend or shorten service life independent of climatic hazard. Consequently, reliable service-life prediction requires both climate-based hazard assessment and appropriate design and protection measures.

The current Australian standard for timber durability classification, AS 5604: 2022 Timber – Natural durability ratings (AS 5604:2022, 2022) classifies above-ground or in-ground durability into four categories i.e. Durability Class (DC) 1 to 4. Each durability class represents a broad probable life expectancy range for the entire country, where climate ranges from temperate to tropical to arid (AS 5604:2022, 2022; BoM 2025). However, AS 5604: 2022 does not incorporate specified regional climatic variability (BoM 2025).

To account for climate influence, the Scheffer Climate Index (SCI) was developed as a measure of above-ground decay potential in the United States based on rainfall and temperature (Carll 2009, Scheffer 1971). While the SCI has been widely used globally for predicting decay hazard (Morris and Wang 2011, Niklewski *et al.* 2016, Wang *et al.* 2007), in Australia, it showed weaker correlation with decay compared to other variables like average vapour pressure deficit (AVPD), suggesting it may not be ideal for Australian climatic conditions or for certain timber species. For example, Francis and Norton (2006) analysed relationships between climate variables and decay data from above-ground L-joint samples of nine species representing the range of durabilities across 11 sites in eastern Australia. They found that AVPD correlated more strongly with decay than SCI or other climate variables such as percentage wet days (PWT) and average evaporation (AE), except for the most durable species, which had minimal deterioration. This is largely because wetted timber tends to dry out more rapidly in the Australian climate, a feature not captured by the SCI. Furthermore, inclusion or exclusion of the only hot, arid site affected correlation strength, highlighting the influence of climatic extremes on decay processes.

Building on the premise that engineering reliability principles could be applied to formulate timber durability design procedures (Leicester and Barnacle 1990) a Forest and Wood Products Australia "Design for Durability" (FWPA DfD) research programme was conceived. Supported by Forest and Wood Products Australia (FWPA) and programme partners, the resulting suite of research outputs included a Timber Service Life Design Guide that incorporated timber service life modelling, drawing upon hazard maps to differentiate decay or termite attack risks throughout Australia (MacKenzie *et al. 2020)*.

The hazard mapping research outlined in this report contributes to addressing the need articulated by MacKenzie *et al.* (2020) to build upon the FWPA DfD programme outcomes.
Focussing on the influence of climate on biodeterioration and using additional field test data, multiple climate-based indices and mapping approaches were assessed to evaluate their suitability for Australian climates. This report contributes to and builds upon these outcomes by evaluating multiple hazard indices for Australian climates, including the SCI, the tentatively-named Department of Primary Industries (DPI) Durability Index (Cause and Carter 1999), and equations

from the FWPA DfD manuals for in-ground (Wang *et al.* 2008a, 2008b, 2008c). Additionally, it explores the development of above-ground hazard maps using a generalised linear model (GLM) that incorporates key climatic variables such as mean annual temperature, average annual vapour pressure deficit, and average daily rainfall.

2. MATERIALS AND METHODS

Australia exhibits highly heterogeneous climatic conditions that strongly influence timber biodeterioration and, consequently, service-life prediction. Unlike the broad nationwide decay classifications provided in AS 5604:2022 (AS 5604:2022, 2022), climatic hazard models capture regional variability driven by differences in rainfall, temperature, humidity, and drying potential. Australia spans tropical and subtropical climates in the north and east, temperate climates in the south, and extensive arid and semi-arid regions inland (BoM Climate Classification Maps, 1991-2020) (BoM 2025).

The workflow began with the compilation of climate data from 140 Bureau of Meteorology (BoM) stations across Australia. These point-based observations were interpolated between stations to create continuous national maps. However, the sparse and uneven spatial distribution of stations resulted in relatively coarse maps with sharp gradients in areas of low station density.

To improve spatial resolution, gridded daily climate data from the SILO (Scientific Information for Land Owners) database, maintained by the Queensland Government, were used. SILO provides high-resolution, interpolated gridded climate data across Australia and allows the calculation of long-term climatic indices (SILO Longpaddock 2025, Stone *et al.* 2019).

Both BoM station-based and SILO gridded datasets were employed to calculate the following indices:

- Scheffer Climate Index (SCI) for above-ground decay hazard,
- DPI Durability Index (DI) for above-ground decay adapted for Australian conditions,
- FWPA Design for Durability climate factors ($k_{climate}$) for both above-ground and in-ground applications, and

Updated above-ground hazard maps developed using a generalised linear model (GLM) that incorporates key climate factors, including mean annual temperature, average annual vapour pressure deficit, and average daily rainfall, and decay lag calculation from field trial data. A comparative analysis was then conducted to assess the behaviour and suitability of each index under Australian climatic conditions.

All decay hazard maps were generated using the R programming environment (Posit Team 2021). Static maps were produced with the *ggplot2* package and Australian shape files, while interactive maps were created using the *leaflet* package.

2.1. Scheffer Climate Index (SCI)

The SCI is a climatic decay hazard index developed to evaluate above-ground decay risk based on temperature and rainfall, with warm and moist conditions being favourable for wood-decaying fungi (Scheffer 1971). The SCI is defined as:

$$SCI = \sum_{Jan}^{Dec} (T-2)(D-3)/16.7 \tag{1}$$

Where T is the mean monthly temperature (°C), and D is the mean number of days in the month with precipitation ≥ 0.25 mm.

The summation is performed over all months of the year. This index is used to classify regions based on their decay hazard potential, with higher values indicating greater decay risk.

The above equation was originally developed for the climate of the USA, where an SCI > 65 was concluded to indicate a severe decay hazard, while an SCI < 35 was considered least favourable for decay. As a general guide, the USA was divided into three hazard areas: 0-35 least conducive to decay; 35-65 intermediate decay hazard; and greater than 65 most conducive to decay. The SCI produces maximum values of around 200 under Australian conditions. To address this (Carter *et al.* 1993), modified the equation to rescale the index to a 0–100 range, as shown below.

$$SCI_{modified} = \sum_{Jan}^{Dec} (T-2)(D-3)/33.2 \qquad (2)$$

SCI values were calculated annually for the period 1987 to 2024 and averaged to create a single composite map for Australia using both data sources (BoM stations and SILO grids).

2.2. DPI Durability Index (DI)

The tentatively-named DPI Durability Index (DI), developed by Cause and Carter (1999) and described in Francis and Norton (2006) extends the SCI approach by incorporating measures of evaporative drying, a dominant driver of decay progression in Australian climates. Unlike SCI, which considers only rainfall and temperature, DI accounts for the evaporative power of the atmosphere following wetting events.

Cause and Carter (1999) demonstrated that indices incorporating rainfall and vapour pressure deficit (VPD – a measure of dryness) correlated more strongly with decay than indices derived from rainfall and temperature alone, as in the SCI. Relatively fewer sites in Australia experience prolonged freezing conditions, as can occur in the United States, where low temperatures may slow decay. Consequently, temperature showed little to no linear or non-linear correlation with decay under Australian conditions (Cause and Carter 1999). DI was calculated as:

$$DI = 2.7278126 - 0.049272315 \times PWT + 0.0431644 \times AVPD \qquad (1)$$

where PWT is percent wet days (% of days with more than 0.25mm precipitation), and AVPD is average vapour pressure deficit (kPa).

The regression coefficients indicated that higher DI values correspond to a lower decay hazard, because increased drying potential (higher VPD) accelerates moisture cycling and fungal activity following wetting events. For the purpose of spatial mapping, (Cause and Carter 1999) inverted and rescaled the regression output to produce a hazard index ranging approximately from 0 to 55:

$$DI_{map} = (\mathrm{DI} \times 100) - 55 \qquad (4)$$

where larger DI_{map} values represent a higher above-ground decay hazard. This transformation does not alter the statistical relationship with climate; it standardises the output for graphical presentation.

In this project, the DI_{map} values were calculated using SILO gridded climate data, providing continuous national coverage and improved spatial resolution relative to station-based calculations.

2.3. FWPA Design for Durability (FWPA DfD) Hazard Maps

The FWPA DfD project developed equations to estimate in-ground and above-ground decay hazard maps, which are described in the following sections (MacKenzie *et al.* 2020, Wang *et al.* 2008a, 2008b).

2.3.1. Above-ground

The derivation of the climate variable for above ground ($k_{cliamte-AG}$) and the estimation of above-ground hazard maps are described in FWPA Design for Durability Manual 4 – Decay above-ground (Wang *et al*. 2008b). In summary, the climate factor is defined as:

$$k_{climate-AG} = \begin{cases} 0.15t_{rain}^{0.5} & \text{if } t_{rain} \text{ is in days/yrs;} \\ 0.03t_{rain}^{0.5} & \text{if } t_{rain} \text{ is in hrs/yrs.} \end{cases} \quad (5)$$

where t_{rain} is the annual time of rainfall.

The 3-hourly rainfall quantity (R_{3hr}) data was used to calculate the effective rainfall duration, t_d, ($t_d = 1.2 + 0.3 ln R_{3hr}$). Summing predicted rainfall duration across all 3-hourly records yields the annual rainfall duration, t_{rain} (hours/year or days/year).

The 3-hourly rainfall quantity (R_{3hr}) was calculated from half hourly rainfall data which is not readily available, in this study, the total rain days per year (number of days of rain more than 0.25mm) was estimated and used to calculate $k_{climate-AG}$ according to **Fel! Hittar inte referenskälla.**.

2.3.2. In-ground

The FWPA DfD Manual 3 – Decay in Ground Contact (Wang *et al.* 2008a) describes the derivation of the in-ground $k_{climate-IG}$ factor as a function of rainfall, temperature, and number of dry months which jointly influence the decay hazard of timber in ground contact. The climate function was expressed as:

$$k_{climate-IG} = f(R_{mean})^{0.3} g(T_{mean})^{0.2} \quad (6)$$

where R_{mean} is the total annual rainfall, and N_{dm} denotes the number of dry months per year (Wang *et al.* 2008a).

A dry month is defined as the month during which the total rainfall does not exceed 5 mm. The function considering the effect of temperature, $g(T_{mean})$, is

$$f(R_{mean}) = \begin{cases} 0 & \text{if } R_{mean} \leq 250 \text{ mm or } N_{dm} > 6, \\ f_0(R_{mean})\left(1 - \frac{N_{dm}}{6}\right) & \text{if } R_{mean} > 250 \text{ mm and } 0 \leq N_{dm} \leq 6 \end{cases} \quad (2)$$

$$g(T_{mean}) = \begin{cases} 0 & \text{if } T_{mean} \leq 5°\text{C}, \\ -1 + 0.2T_{mean} & \text{if } 5 < T_{mean} \leq 20°\text{C}, \\ -25 + 1.4T_{mean} & \text{if } T_{mean} > 20°\text{C}. \end{cases} \quad (3)$$

and

$$f_0(R_{mean}) = 10\left[1 - e^{-0.001(R_{mean}-250)}\right] \tag{4}$$

where T_{mean} is the mean annual temperature.

The maps calculated from the above equations were subsequently refined using expert judgement as shown in Figure *1*.

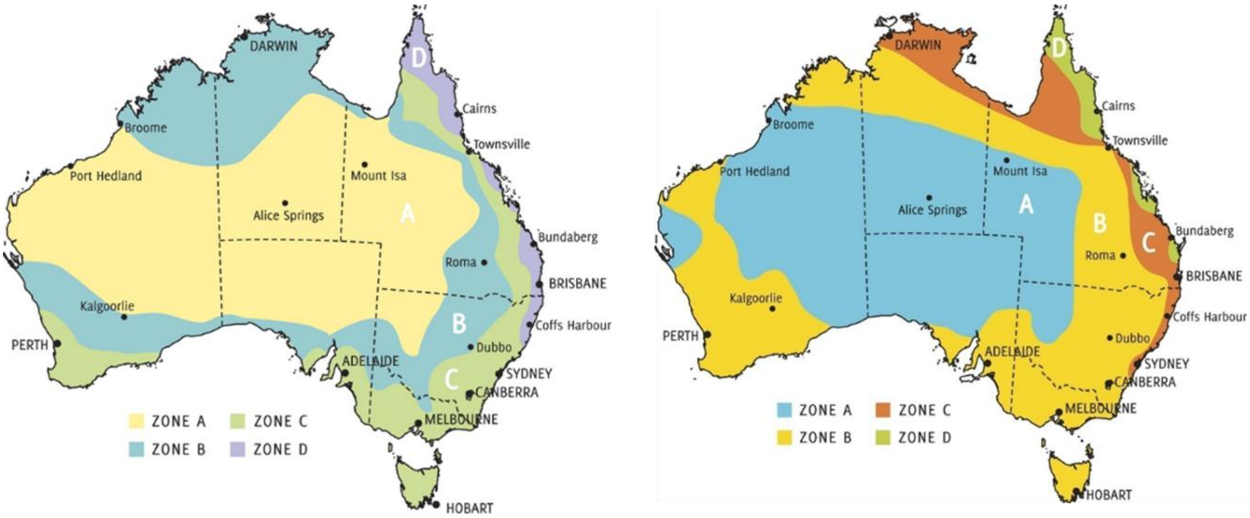

Figure 1: Modified above-ground (left) and the in-ground (right) hazard maps from the Design for Durability project.

The $k_{climate}$ values for in ground and above ground models are given in Table 1.

Table 1: $\boldsymbol{k_{climate}}$ values for in ground and above ground models (Wang *et al.* 2008a, 2008b).

Hazard Zone	**Above-ground** $k_{climate-AG}$	**In-ground** $k_{climate-IG}$
A	0.40	0.5
B	0.50	1.5
C	0.65	2.5
D	0.75	3.0

2.4. Updated Above-ground Hazard Maps using GLM and Field Data

To enhance the existing climate hazard maps for above-ground applications, L-joint field data collected between 1987 and 2024 from eleven sites were analysed to evaluate the influence of key climate variables on decay lag and to establish correlations with Australia's diverse landscape. Detailed information on the site locations, as well as the data collection and processing methods, is available in Wang *et al.* (2008b)

The dataset included eight timber species under two paint conditions (painted and unpainted) across eleven sites. For each species × paint × site combination, 21 replicate samples were installed and monitored, resulting in a total of 3696 samples. Out of these samples, 2872 presented some level of decay (allowing decay lag to be calculated; i.e., the number of years before the onset of visible decay), whilst decay rate (mm/y) was only able to be calculated for 1869 samples, due to many of the samples not having reached failure before the trial's completion (thus prohibiting rate calculations). Moreover, decay rate was unable to be estimated for some species, paint and site combinations, which restricted accurate modelling functions. To account for the low-rate sample size, a formula was developed to estimate rate as a function of decay lag (when rate data did not exist), based on the relationships between rate and lag for samples with rate data. This formula is outlined in Equation 9.

$$Rate = \frac{3.62}{Lag} \tag{5}$$

where $Rate$ is decay rate (mm/y) and Lag is decay lag (years).

A generalised linear model (GLM) was developed to estimate decay rate (as calculated in Equation 10) as a function of wood species, paint condition, and climate. GLM frameworks have been consistently employed in timber durability modelling (e.g., Carter *et al.* 1993, McBride and Nicholls 1983, Ohnesorge *et al.* 2010) as they can account for right skewness (as decay is considered to only be non-negative) and heteroskedasticity (since decay can vary greatly in time and space and between different species and coatings). All available climate variables from the SILO dataset were processed, including temperature-related variables (minimum, maximum, and mean), humidity (minimum, maximum, and mean), vapour pressure, rainfall variables (total rainfall, number of rain days, and dry days), radiation, and evaporation. These variables were extracted for each site. However, only three key climate variables - mean annual temperature, average annual vapour pressure deficit, and average daily rainfall - were included in the modelling framework. This selection was based on their significant and varying influence on timber decay and to minimise redundancy and multicollinearity in the analysis. The GLM used a Gamma error distribution with a log link to account for the strictly positive, right-skewed distribution of durability lag. By exponentiating the model coefficients, species, paint, and climate variables act as multiplicative factors (k-values), allowing coefficients to be interpreted directly as proportional effects on decay rate. The GLM formulation was as follows:

$$log(Rate) = \beta 1 \cdot Wood + \beta 2 \cdot Paint + \beta 3 \cdot MeanTemp + \beta 4 \cdot AvgDailyRain + \beta 5 \cdot VPD \tag{6}$$

where $Rate$ is annual decay rate (mm/y); $Wood$ is the AS5604:2022 timber durability class (unpainted); $Paint$ is the adjustment factor for painted samples; $MeanTemp$ is the average annual mean temperature (ºC); $AvgDailyRain$ is average daily rain (mm/day); and VPD is the average vapour pressure deficit (kPa).

Exponential transformation of the coefficients in Equation 10 allowed decomposition of the expected degradation rate into multiplicative components (k-values), as outlined in Equation 11. Derivation of each k-value (k_{wood}, k_{paint} and $k_{climate}$) is provided in Equations 12 to 14.

$$Rate = \frac{3.62}{Lag} = k_{wood} * k_{paint} * k_{climate} \tag{7}$$

$$k_{wood} = \exp\,(\beta 1 \cdot Wood) \tag{12}$$

$$k_{paint} = \exp\,(\beta 2 \cdot Paint) \tag{13}$$

$$k_{climate} = \exp\,(\beta 3 \cdot MeanTemp + \beta 4 \cdot AvgDailyRain + \beta 5 \cdot VPD) \tag{14}$$

where $Rate$ is annual decay rate (mm/y); k_{wood} is the AS5604:2022 timber durability class parameter (unpainted); k_{paint} is the paint parameter for each species; and $k_{climate}$ is the climate parameter (and a function of mean temperature, daily rainfall and vapour pressure deficit). This paper focusses primarily on the results of $k_{climate}$.

A spatially explicit hazard map was finally developed based on the $k_{climate}$results from the GLM coefficients, and applied to gridded climate data from the SILO (Scientific Information for Land Owners) database.

3. RESULTS AND DISCUSSION

3.1. Scheffer Climate Index (SCI)

Figure *2* presents the SCI for four selected years, illustrating that SCI varies in response to climate variability. Climate variability also driven by large-scale ocean-atmospheric influences including the El Niño-Southern Oscillation (ENSO). El Niño phases are typically associated with below-average rainfall and warmer conditions across eastern Australia, whereas La Niña phases produce above-average rainfall, increased cloud cover and cooler, wetter conditions (McBride and Nicholls 1983). Because long-term durability trials used to calibrate climatic indices were primarily conducted in eastern Australia, ENSO cycles occurring within the 1987-2024 period are expected to have influenced both measured decay behaviour and model outputs.

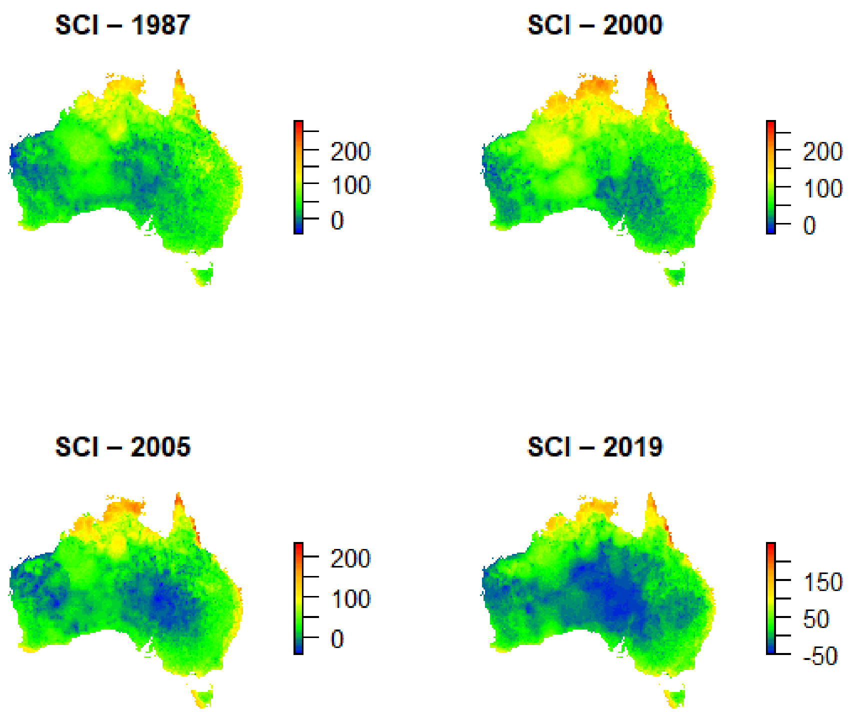

Figure 2: Scheffer Climate Index (SCI) for Australia for selected years: 1987 (closer to average rainfall), 2000 (above average rainfall), 2005 (closer to average rainfall) and 2019 (below average rainfall).

To generalise the decay hazard across 1987 to 2024 – the period over which L-joint test data are available – Figure *3* shows the average SCI index using the unmodified Scheffer equation.

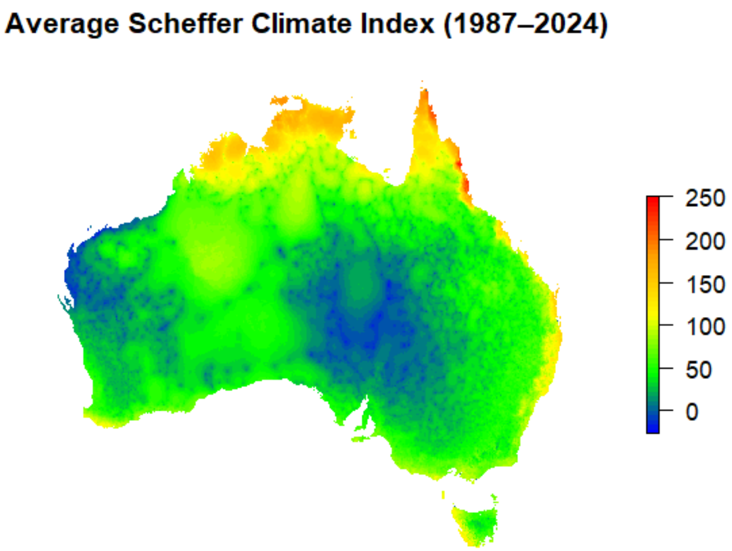

Figure 3: Average SCI (1987–2024) using raw equation including negative values.

It is also important to note that SCI values can become negative when the mean monthly temperature falls below 2 °C or when the number of wet days in a month (precipitation ≥ 0.25 mm) is fewer than three.

The average map produced in this report differs from the SCI map presented in the FWPA DfD Manual (Wang *et al.* 2008b) because the calculation period here spans an extended range and includes multiple high-rainfall La Niña years. The end of the period coincided with a prolonged positive ENSO phase, resulting in record rainfall and widespread flooding across eastern Australia (Huang *et al.* 2024). Consequently, the long-term SCI in northern and eastern regions is higher than historical estimates.

Figure *4* shows the average SCI using the modified formula (Eq. 2), which is similar to Figure *3* but in a different scale.

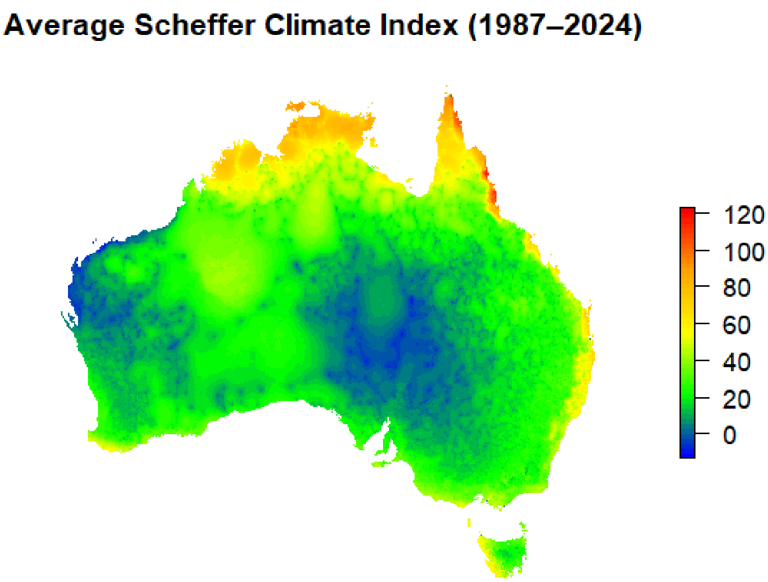

Figure 4: SCI average of all years from 1987-2024 using the equation for Australia.

3.2. DPI Durability Index (DI)

The DPI Durability Index (DI) (Cause and Carter 1999, Francis and Norton 2006) is inversely related to decay hazard, meaning that lower DI values correspond to higher above-ground decay risk, while higher DI values indicate lower hazard. This relationship applies to the original DI formulation, without being inverted and rescaled to produce mapped values in the range of 0-55 for graphical presentation. The DI captures the accepted decay hazard in southern Western Australia but may overestimate the decay hazard in Tasmania (Figure *5*). While there are anecdotal reports of high decay hazards in Tasmania, this region is unlikely to be more severe than the tropics, and it is likely that this index may be overestimating the decay hazard for this region due to local climatic or data-interpolation effects. As a result of this finding, additional field trials will be established to further explore climate effects an provide additional data for modelling as part of this project.

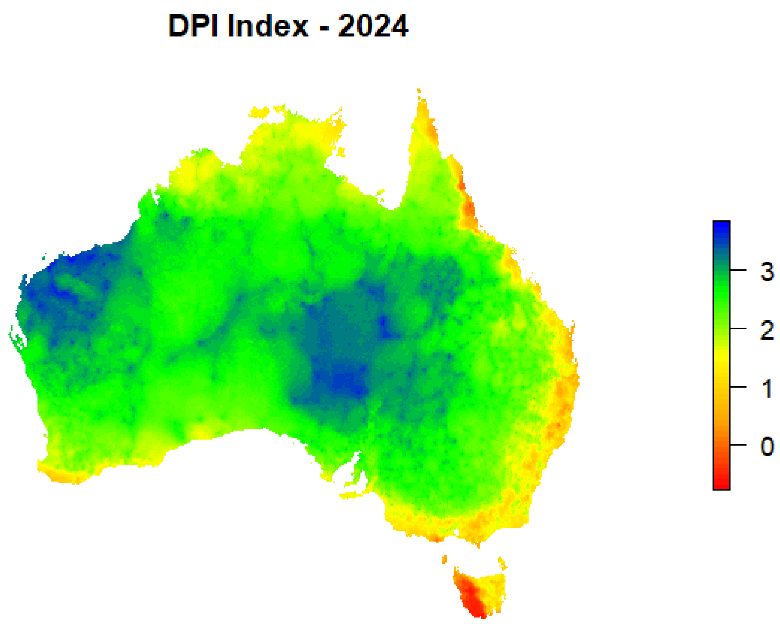

Figure 5: DI for a selected year (2024).

Figure *6* shows the average DI between years 1987 to 2002 (to compare and validate with the values reported in Francis and Norton (2006)) and 1987 to date (L-joint exposure duration). The average DI for 1987-2002 displays a pattern consistent with earlier studies by Francis and Norton (2006) confirming that the index effectively captures regional climatic influences on above-ground decay. High-hazard zones (low DI values) remain concentrated in tropical and subtropical areas, while low-hazard zones (high DI values) dominate central inland Australia.

This may reflect long-term climatic drying trends and increased evaporative potential observed in more recent decades. The broader spatial coverage of the SILO gridded data (1987-2024) also reduces local artefacts and enhances the smoothness of the interpolated surfaces, improving the consistency of hazard classification relative to earlier, station-based datasets.

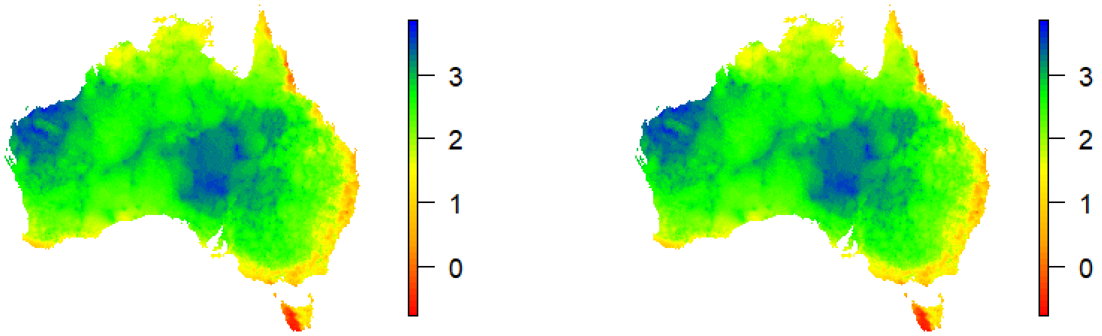

Figure 6: Comparison of average DI for 1987-2002 (left) and 1987-2024 (right).

3.3. FWPA Design for Durability (FWPA DfD) Hazard Maps

While the Scheffer's Climate Index and DPI durability index were developed to characterise above-ground decay hazard, the FWPA DfD project produced climate-based hazard maps for both above-ground and in-ground exposures. These maps draw on the climate factor, which was derived using rainfall duration, temperature, and dry-month metrics, depending on the in-ground or above-ground exposure. The maps generated in this report provide continuous high resolution spatial values than discrete hazard zones reported in FWPA DfD manuals (Wang *et al.* 2008a, 2008b). The hazard zones will be assigned in subsequently drawing upon insight from updated data and expert opinion.

3.3.1. Above-ground

Figure *7* presents the calculated $k_{climate-AG}$ values for the above-ground exposure, based on time-of-rainfall data reported in Appendix B of the FWPA Above-Ground Manual 4 (Wang *et al.* 2008b). The results show markedly higher $k_{climate-AG}$ values at northern Queensland sites such as South Johnstone and Innisfail, where values exceed 1.0. In contrast, the Timber Service Life Design Guide (MacKenzie *et al.* 2020) treats Brisbane and northern Queensland as the same climatic zone. However, the site-specific calculations presented here highlight meaningful differences; Brisbane exhibits, $k_{climate-AG} \approx 0.74$, compared with ≈ 1.10 at Innisfail. This suggests that the zone-based approach may underrepresent the climatic severity for some high-rainfall locations in the tropics.

As noted by Scheffer (1971), zonal maps provide broad guidance, whereas formula-based calculations offer a more precise basis for design considerations or the required preservative treatment needed for above-ground wood exposed to weather.

A limitation of the Design for Durability $k_{climate-AG}$ above-ground formula, is its reliance on half-hourly rainfall data, which are scarcely available from BoM and pose much uncertainty due to the lack of distinction between missing data and the absence of rain. The original FWPA work used limited hourly BoM datasets. Current work has shifted toward using SILO data, which benefit from interpolation to address missing BoM observations; however, SILO rainfall is provided only as daily totals, reducing temporal resolution. The SILO interpolated data do not include hourly rainfall, and many BoM stations have incomplete hourly rainfall records, making it difficult to generate interpolated national maps.

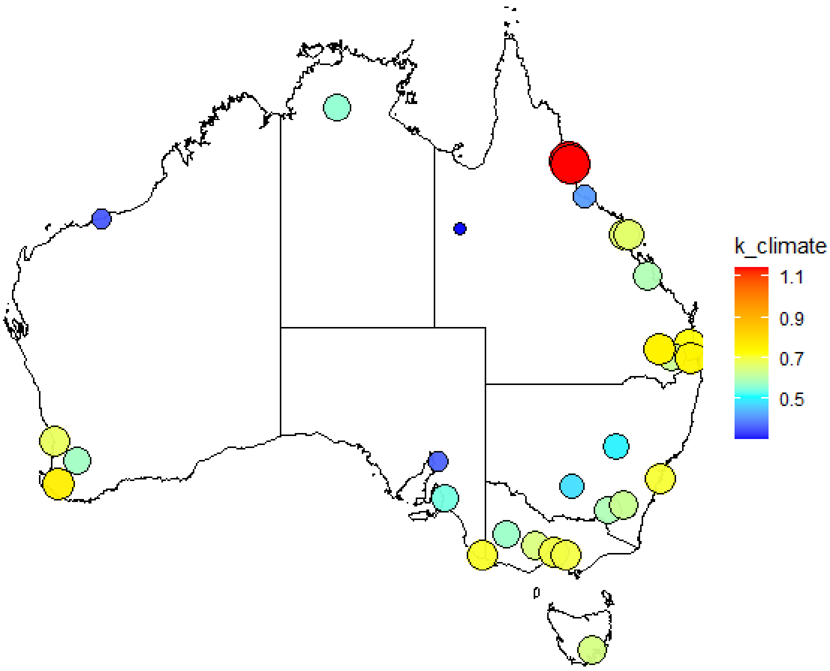

Figure 7: Site-based $k_{climate}$ values for L-Joint and Panel Test sites, with point size and colour scaled to magnitude.

Because many BoM stations had incomplete hourly rainfall records, a fully continuous national map could not be produced. Nevertheless, an interpolated surface based on the available test sites provides a coarse indication of spatial variability across Australia. While the interpolation highlights broad patterns, the resolution remains limited by the number and distribution of test sites. To supplement these coarse patterns, a second interpolation (Figure 8) was produced using BoM station-based calculations of t_{rain} and $k_{climate-AG}$. While still constrained by data gaps, this broader dataset offers a more representative overview of climatic gradients at the continental scale and will be refined further using SILO inputs in future analyses.

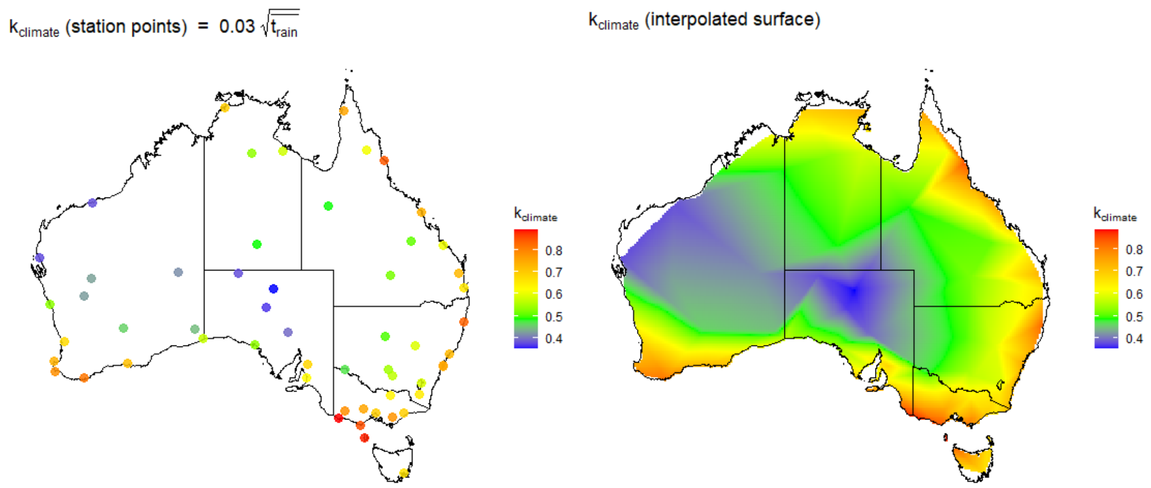

Figure 8: $k_{climate-AG}$ at field test site location (left) and interpolated map (right) derived from $\boldsymbol{t_{rain}}$ values reported in appendix B of Manual 4 (Wang *et al.* 2008b).

The effective rainfall duration t_d and then time of rainfall, t_{rain} is more difficult to obtain than simpler rainfall metrics (e.g., total annual rainfall or number of wet days, defined as days with ≥ 0.25 mm precipitation). Hourly rainfall data are available for some sites, but half-hourly resolution would be preferable for accurate estimation. In the previous DfD project, the datasets used were limited to one or two years (2000-2001) for nine cities, which may not be representative of long-term or nationwide conditions.

Additionally, some purchased hourly datasets contained missing values (for example, the Brisbane station data were only complete for January–February 2000. Therefore, an alternative approach was developed in this project to estimate $k_{climate-AG}$ for above ground exposure using more accessible parameters i.e. number of rain days.

The above-ground climate hazard map generated using the annual number of rain days is shown below in Figure 9. The method indicates a comparatively higher above-ground hazard in western Tasmania, primarily due to the region's large number of rain days. However, this elevated hazard level may not fully reflect true decay risk. Western Tasmania is characterized by frequent light rainfall but relatively cool temperatures, and temperature may affect fungal decay activity. Because temperature was not included in the current calculation, the hazard in this region may be overestimated. Despite the potential regional overestimations, the magnitude of $k_{climate-AG}$ produced using rain days ranges from 0 to 3. These values are now consistent with the magnitudes observed for in-ground (IG) hazard indices and represent an improvement over the previous above-ground range of 0.4-0.75, which showed limited variation.

The broader spread of values obtained with the new method may therefore provide a more realistic differentiation of above-ground decay hazard across Australia. To address potential overestimation in cooler, high-rainfall regions such as Western Tasmania, future work will incorporate a temperature-based adjustment factor into the $k_{climate-AG}$ equation. Including both rainfall frequency and thermal conditions is expected to yield a more accurate representation of above-ground decay potential.

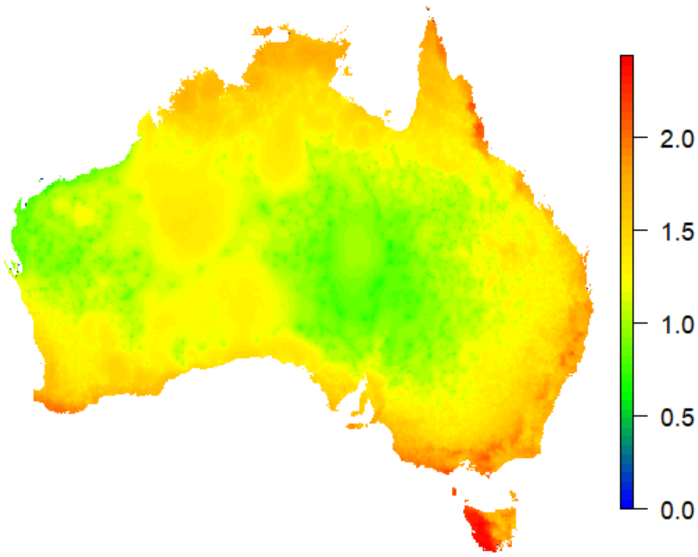

Figure 9: $k_{climate-AG}$ values from SILO data for average value between year 1987 to 2024.

3.3.2. In-ground

Figure 10 presents the $k_{climate-IG}$ values, both as point observations from 144 BoM weather stations and as an interpolated heatmap. The heatmap displays some sharp boundaries, which result from the relatively coarse spatial distribution of climate stations and the limited density of available data points in certain regions. To address this limitation and improve spatial continuity, gridded data from SILO was again employed, which allowed the generation of smoother and more reliable $k_{climate-IG}$ maps.

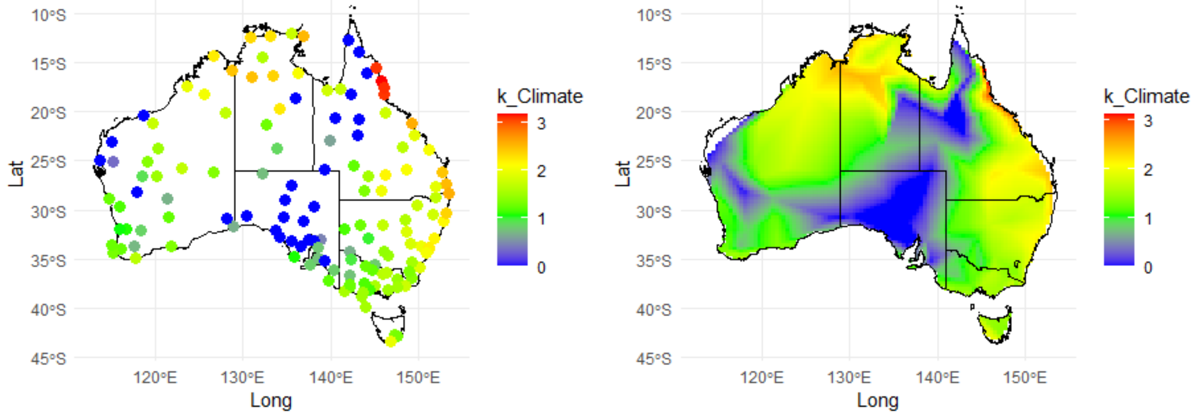

Figure 10: Interpolated $k_{climate-IG}$ values from station data (left) and interpolated data from 144 BOM station on (right) for 2024.

Figure *11* shows $k_{climate-IG}$ for selected individual years within the duration of the stake test (1) which was drawn upon for modelling (Wang *et al.* 2008a) and Figure 12 shows average $k_{climate-IG}$ values from all years between 1968 and 2000. It shows that $k_{climate-IG}$ can vary significantly between years, influenced by variation in climate drivers.

According to the equations described in Section 2.3.2, the in-ground climate factor ($k_{climate_{IG}}$) becomes zero under certain climatic conditions. Specifically, when the mean annual rainfall (R_{mean}) is less than or equal to 250 mm, the mean dry-month number (N_{dm}) exceeds 6, or the mean annual temperature (T_{mean}) is less than or equal to 5 °C, the equations or model predicts no decay activity. The model implies that the decay rate would be zero under such climatic conditions, which may not reflect real-world conditions, as some level of biological decay may still occur, even in cold or dryer environments. The formulation will be further considered in the future when additional climatic and decay data become available. However, average $k_{climate-IG}$ over muiltiple years (e.g. Figure 12) provides a more generalised of climate hazard.

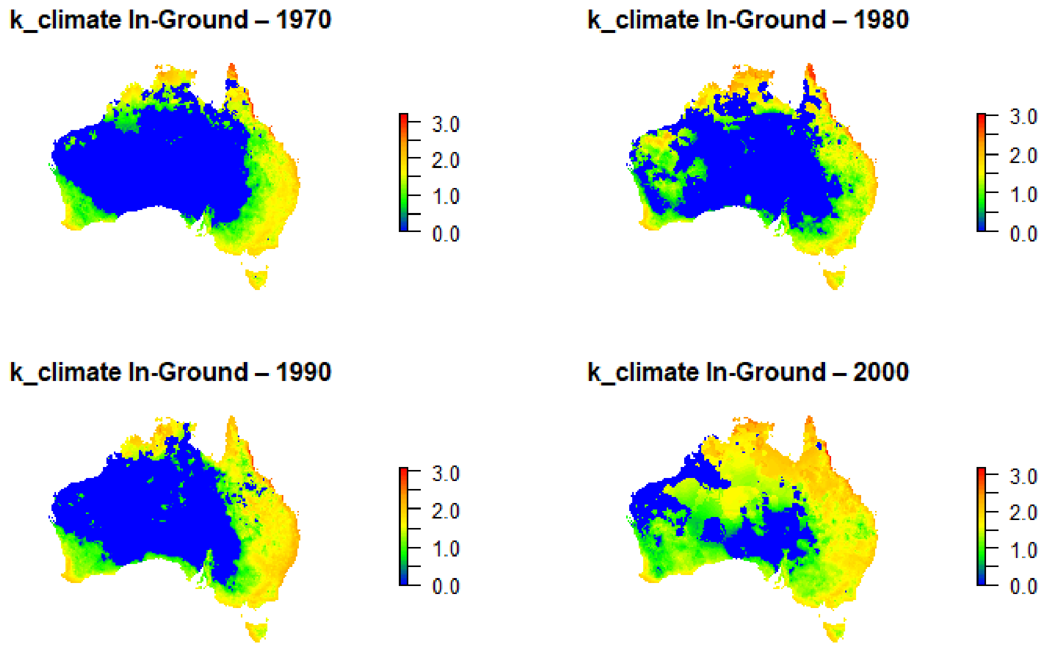

Figure 11: $k_{climate-IG}$ values from SILO data for four selected years, illustrating interannual variability associated with major climate cycles.

These annual maps illustrate consistent spatial patterns through time, with relatively stable high-hazard zones in the tropical north, along eastern coastal regions, and low-hazard zones across the arid interior and central west of Australia. Minor inter-decadal changes correspond to climatic variability associated with major rainfall cycles previously mentioned. For example, the map shown in Figure *11* for year 2000 was amid an ENSO La Niña event with above-average rainfall.

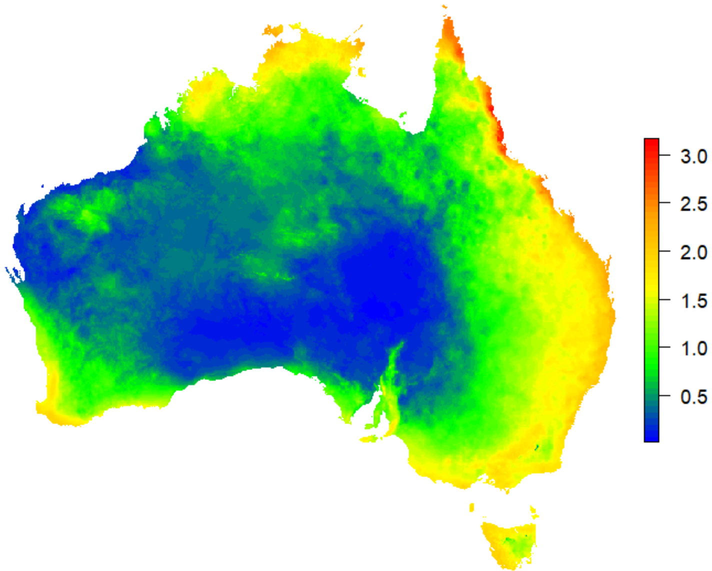

Figure 12: Average $k_{climate-IG}$ values from SILO data for 1968-2000.

Existing in-ground field test datasets are confounded by simultaneous termite attack and decay. Unfortunately, data from the FWPA DfD project Stake Test 2, which included stake sets treated only with an insecticide to separate decay and termite attack, are no longer available. To address this gap, a new field trial of pine sapwood, including insecticide-treated replicates, will be established nationally to generate clean decay-only datasets for improved model calibration. These data will assist with calibration of updated modelling that is underway.

3.4. Above-ground Hazard Maps Derived from Field Data

The results of the Generalised Linear Model (GLM) for the calculation of $k_{climate}$ are presented in Equation 15, which outlines the coefficients for each independent variable included in the regression analysis.

$$k_{climate} = \exp\left(0.012 \cdot MeanTemp - 0.020 \cdot AvgDailyRain + 0.018 \cdot VPD\right) \qquad Eq.\ 8$$

Figure *13* presents average above-ground $k_{climate}$ derived from the L-Joint decay rate data from 1987 to 2024 and gridded climate data from the SILO. Higher $k_{climate}$ represents higher annual rates of timber decay. With the inclusion of mean annual temperature, mean daily rainfall and average annual VP deficit, the climate hazard maps improve upon the SCI (which only consider mean temperature and mean number of days with precipitation) and DI (which considers the percent of wet days and average VP deficit) climate hazard maps.

Decay rate was positively correlated with mean temperature and rainfall and negatively correlated with VP deficit. As such, areas of high decay include north-east Queensland (due to its high temperature and rainfall and low VP deficit), and Western Tasmania (high rainfall and low VP deficit), whilst areas in central Australia experience low decay rate despite its high temperature, due to the lower VP deficit and rain. Nonetheless, as shown in Figure *13*, changes in climate variables can greatly impact predicted rates of decay. This should be closely considered for future field applications due to future global climate change forecasts.

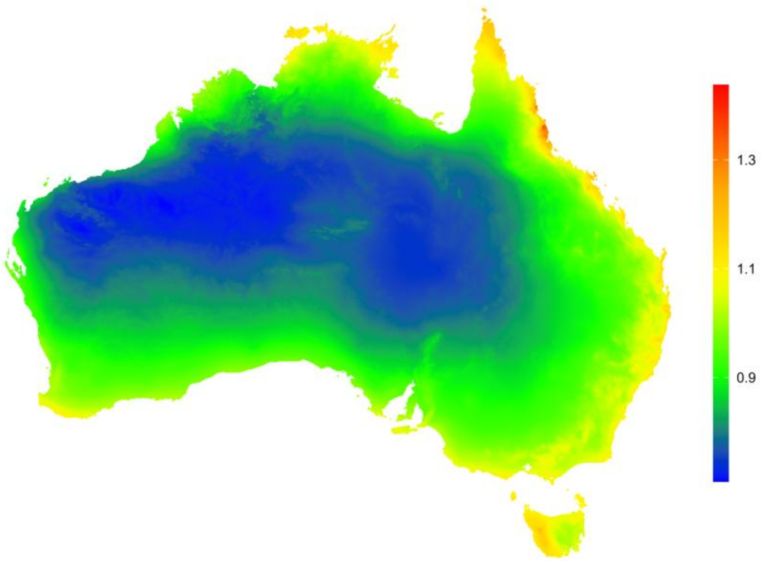

Figure 13: $k_{climate}$ average of all years from 1987-2024, as derived from the GLM formulation.

Despite the hazard map improvements on the preliminary decay models, its predictive strength is constrained by a relatively small dataset and the limited climatic spread of the underlying data (with most samples having been installed in coastal locations in Eastern Australia). Richer datasets spanning broader environmental gradients would strengthen parameter estimation, reduce uncertainty, and improve the robustness of the model. For many species, paint and site combinations, decay rate did not exist. In these circumstances, rate was estimated as a function of lag (Equation 9). Expanded datasets would provide opportunities to model decay rate more accurately and help validate the $k_{climate}$ estimates.

4. CONCLUSIONS

Decay hazard maps for Australia were developed using multiple approaches and their comparative overview and discussion of their outcomes were presented. Each hazard mapping approach reviewed had strengths and weaknesses. For example, the SCI may underrepresent the decay potential in southern WA and regions near but not very close to the coast. The DI captures WA but may overestimate Tasmania. Both of these indices were developed to summarise decay hazards above-ground. FWPA DfD maps summarise decay above- and in-ground. Zoned hazard maps can present helpful generalisations to identify decay risk, however, abrupt changes near the boundaries can over or underestimate decay rate.

To address limitations of zonal maps, freely available SILO climate data was used to refine and enhance the FWPA DfD hazard maps. Higher-resolution decay hazard maps for both in-ground and above-ground environments were produced, based on $k_{climate}$ values, with smoother transitions across boundaries and interactive capability. The challenges associated with applying the current equations presented in the FWPA DfD for both in-ground and above-ground applications are discussed. While the in-ground maps appear realistic, deriving above-ground hazard maps based on rainfall duration remains challenging due to current data limitations. To address this, a new method utilising a generalised linear model (GLM) and field trial data was introduced, resulting in an improved above-ground hazard map informed by field data. While maps and formulae need to be provided in the context that building design considerations (including levels of weather exposure, maintenance, avenues for water ingress or egress), variability in biodeteriogens (which would benefit from future studies) and inconsistent climatic conditions over time, limit the level of long-term specificity that predictions can offer, they provide information that is superior to blanket wide-ranging classifications throughout Australia.

5. ACKNOWLEDGEMENT

The authors gratefully acknowledge the financial support provided by Forest and Wood Products Australia through the National Centre for Timber Durability and Design Life (NCTDDL), hosted by the University of the Sunshine Coast. The Queensland Department of Primary Industries is also acknowledged for its financial and technical support, including access to research facilities and resources at the Salisbury Research Facility in Brisbane. The authors extend their sincere thanks to the FWPA Design for Durability Project Team (Bob Leicester, the late Colin MacKenzie, Chi-hsiang Wang, Minh Nguyen, Greg Foliente and their research teams) for their valuable contributions. The authors also sincerely thank the project steering committee for their constructive feedback and guidance throughout the study. Steering committee members included Andrew McLaughlin (AKD), Bill Leggate (Griffith University; formerly Queensland DPI), Christian Brischke (Thünen Institute, Germany), Harry Greaves (HG Consulting), Ian Blanden (Forest and Wood Products Australia), Jeff Morrell (University of South Australia), Keith Crews (University of Queensland), Kyra Wood (University of Tasmania), and Tripti Singh (University of the Sunshine Coast / National Centre for Timber Durability and Design Life).

6. REFERENCES

AS 5604:2022 (2022): AS 5604:2022 Timber - Natural durability ratings. *Standards Australia*, **30**. www.standards.org.au

BoM (2025): Climate classification maps. *Bureau of Meteorology, Commonwealth of Australia. accessed 6 November 2025*. https://www.bom.gov.au/climate/maps/averages/climate-classification/?maptype=kpngrp.

Carll, C G (2009): *Decay hazard (Scheffer) index values calculated from 1971-2000 climate normal data*. http://dx.doi.org/10.2737/FPL-GTR-179

Carter, J O, Cause, M, Moffat, A (1993): *A preliminary above-ground wood decay index map of Australia*.

Cause, M L, Carter, J O (1999): Above-ground wood decay index map. *Milestone Report, Department of Primary Industries*.

Eaton, R A, Hale, M D (1993): *Wood: decay, pests and protection*. Chapman and Hall, London.

Francis L, Norton J (2006): Predicting the decay resistance of timber above-ground: 1. Climate effects. *Proceedings IRG Annual Meeting,* IRG/WP 06-20330.

Huang, A T, Gillett, Z E, Taschetto, A S (2024): Australian rainfall increases during multi-year La Niña. *Geophysical Research Letters*, **51**(9), e2023GL106939.

Leicester, R H, Barnacle, J E (1990): Durability - a structural approach

MacKenzie, C, Wang, C, Leicester, R, Foliente, G, Nguyen, M (2020): Timber service life design. Design guide for durability (First produced December 2007, revised 2012, 2013, 2015, 2020). *Forest and Wood Products Australia Limited*.

McBride, J L, Nicholls, N (1983): Seasonal relationships between Australian rainfall and the Southern Oscillation. *Monthly Weather Review*, **111**(10), 1998-2004.

Morris, P, Wang, J (2011): Scheffer index as preferred method to define decay risk zones for above ground wood in building codes. *International Wood Products Journal*, **2**(2), 67-70.

Niklewski J, Hansson E F, Brischke C, Kavurmaci D (2016): Development of decay hazard maps based on decay prediction models. *Proceedings IRG Annual Meeting,* IRG/WP 16-20588, 14 pp.

Ohnesorge, D, Richter, K, Becker, G (2010): Influence of wood properties and bonding parameters on bond durability of European Beech (*Fagus sylvatica* L.) glulams. *Annals of Forest Science*, **67**(6), 601-601.

Posit Team (2021): RStudio: Integrated development environment for R. *Posit Software, PBC, Boston, MA. URL http://www.posit.co/.*

Rayner, A D, Boddy, L (1988): *Fungal decomposition of wood. Its biology and ecology*. John Wiley & Sons, Ltd., Chichester.

Scheffer, T (1971): A climate index for estimating potential for decay in wood structures above ground. *Forest Products Journal*, **21**(10), 25-31.

SILO Longpaddock (2025): Climate data *accessed 2025 https://www.longpaddock.qld.gov.au/silo/.*

Stone, G, Pozza, R D, Carter, J, McKeon, G (2019): Long Paddock: climate risk and grazing information for Australian rangelands and grazing communities. *The Rangeland Journal*, **41**(3), 225-232.

Wang, C, Leicester, R, Nguyen, M (2008a): Manual 3 – Decay in ground contact. In: Forest and Wood Products Australia Limited.

Wang, C, Leicester, R, Nguyen, M (2008b): Manual 4 - Decay above ground. In: Forest and Wood Products Australia Limited.

Wang, C, Leicester, R, Nguyen, M (2008c): Manual 11 - Equations for Use in a Service Life Design Guide. *Forest and Wood Products Australia Limited*.

Wang J, Wu X, Jiang M, Morris P, Wang J, Wu X, Jiang M, Morris P (2007). Decay hazard classifications in China for exterior above-ground wood. *Proceedings IRG Annual Meeting,* IRG/WP 07-20357, 10 pp.

Zabel, R A, Morrell, J J (2020): *Wood microbiology: decay and its prevention*. Academic press.